



β Zeolite/bentonite composite as a novel catalyst for condensation of aniline to diphenylamine

Yeqing Yang¹ · Yingling Liao¹ · Naiwang Liu¹ · Li Shi¹ · Xuan Meng¹

Accepted: 5 August 2021 / Published online: 5 September 2021

© The Author(s), under exclusive licence to Springer Science+Business Media, LLC, part of Springer Nature 2021

Abstract

β Zeolite/bentonite composite was synthesized by simple kneading as catalyst for condensation reaction of aniline to diphenylamine. The experiment which was conducted at 320 °C under 2 MPa with a liquid hourly space velocity (LHSV) of 2 h⁻¹ showed that the H β zeolite loading 25% clay exhibited the highest activity (9.9% aniline conversion) and selectivity. Pilot experiments (315–320 °C, 2 MPa, LHSV of 0.20–0.22 h⁻¹) have also confirmed that the catalyst had good stability. The crystalline structure, acidic property and textural property of the catalysts were characterized by XRD, Py-IR, N₂ adsorption–desorption. Moreover, according to the thermodynamic analysis, the condensation of aniline to diphenylamine is an exothermic reaction, indicating that too high temperature operation is unfavorable for the reaction. The studied β zeolite/bentonite composite is of promising efficiency in condensation of aniline to diphenylamine.

Keywords β Zeolite · Bentonite · Aniline · Condensation · Diphenylamine

1 Introduction

Diphenylamine (DPA), also known as phenylaniline, is widely used in industry [1]. It can be used to synthesize rubber antioxidants, fuels and pharmaceutical intermediates, lubricating oil antioxidants, and is also a gunpowder stabilizer. As the continuous expansion of the application field of diphenylamine, *p*-amino diphenylamine, a derivative of diphenylamine, is the basic raw material of *p*-phenylenediamine antioxidants.

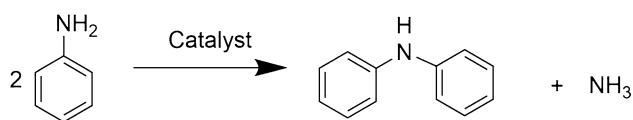
The main synthetic routes of diphenylamine include aniline-phenol condensation method, aniline batch synthesis method, and aniline continuous synthesis method [2–5]. The current method of synthesizing diphenylamine is mainly the continuous liquid phase self-shrinking method of aniline (Scheme 1). In term of reaction condition, it was wilder than others. Furthermore, compared with other routes, it has advantages in conversion and selectivity. The key to the improvement of the synthesis process lies in the catalyst. Numerous experimental data indicate that this condensation

reaction requires a certain acidity of the catalyst. In the beginning, most manufacturers adopted the batch method, with AlCl₃ as the catalyst. The biggest disadvantage of this method is that the catalyst is very corrosive to the equipment and is not conducive to continuous production.

At present, the acid catalyst used for continuous liquid phase condensation in industry is mainly β zeolite. β zeolite is the molecular sieve with three-dimensional twelve-membered ring channels [6]. Meanwhile, it has crossing channels and no cage structure. In addition, there are a lot of lattice defects and open pores in the β zeolite. This unique topology structure has unique surface properties and catalytic activity, and has a very wide range of applications in the field of catalysis. Hronec et al. [1] employed β zeolite with different Si/Al atomic ratio to investigate the condensation of aniline to diphenylamine and found that β zeolite with higher Si/Al atomic ratio was less active. β zeolite was also used in gasoline cracking reaction [7], dehydration of glycerol [8] and so on. However, the ratio of β -zeolite framework to silica-alumina is relatively small, and the microporous structure of β zeolite will affect the diffusion of intermediate products and delay the reaction. Bochkarev et al. [5] have supposed that the condensation reaction can form the *p*- σ complex intermediate through the exploration of the reaction mechanism and quantum chemistry calculations. Therefore, in order to achieve higher conversion and yield, it

✉ Xuan Meng
mengxuan@ecust.edu.cn

¹ International Joint Research Center of Green Energy Chemical Engineering, East China University of Science and Technology, Shanghai 200237, China



Scheme 1 The condensation reaction of aniline to diphenylamine

is necessary to modify the β zeolite to improve the catalytic activity and stability of the β zeolite [9–13]. To the contrary of the microporous structure of β zeolite, the mesoporous structure of clay is conducive to the diffusion of intermediate products.

Clay is mainly composed of bentonite. Montmorillonite is a layered aluminosilicate mineral containing water [6, 14–17], and its basic structural unit is a TOT layered structure, the sheets are connected by a common oxygen atom. Due to its acidity, it can often be used as a carrier for acidic catalysts. In addition, montmorillonite is a mesoporous material with a large specific surface area and porosity. In recent years, many researchers have produced novel hybrid material between raw bentonite and zeolite in order to improve the performance of the catalyst. Bentonite/zeolite-NaP composite was synthesized by Shaban et al. [18], and showed high removal efficiency for methylene blue. Abukhadra et al. [19] successfully prepared the bentonite/zeolite hybrid and found that the hybrid structure is of excellent recyclability properties and is of promising efficiency in reducing Sr(II) and U(VI) from the groundwater sample. Unfortunately, the research about the application of the composite from bentonite and β zeolite has not been investigated yet.

Therefore, in this work, a novel composite of β zeolite/bentonite will be synthesized as a catalyst, which can not only adjust the acidity, but also enrich the distribution of catalyst pores and help the transfer of intermediate species in the reaction. The purpose of this paper is to evaluate the catalytic performance of aniline. The study also involved detection of optimal loading capacity of clay and thermodynamic studies.

2 Experimental

2.1 Catalyst preparation

$\text{NH}_4\beta$ zeolite (Si/Al = 25) was obtained from Nankai University Catalyst Co., Ltd. The clay was purchased from Shanghai Aladdin Biochemical Technology Co., Ltd. The catalysts were prepared by mixing and kneading. First, the clay of different qualities (mass fractions of 25%, 35%, and 50%, respectively) were mixed with H β zeolite until the catalyst was formed. The catalyst mixed with Al_2O_3 (10%) as binder and HNO_3 as peptizer were extruded into strips.

Afterwards, the catalysts were dried overnight at 110 °C and calcined at 550 °C for 4 h to remove the occluded organic species. The catalyst obtained were named H β , H β -25, H β -35, H β -50 and clay. All samples were screened into 20–40 mesh for use.

2.2 Catalytic performance

Catalytic tests were carried out in a fixed-bed tubular reactor with 3 ml of the catalyst (inner diameter 6 mm). Quartz sand were added to the upper and the lower part of the constant temperature section to prevent the quartz sand from rushing out when N_2 is purged. Schematic view fixed-bed tubular reactor for the liquid phase conversion of aniline to diphenylamine was shown in Fig. 1. Aniline and diphenylamine were obtained from Sinopharm chemical reagent. The liquid hourly space velocity (LHSV) of aniline was set at 2 h^{-1} as the reaction was carried out at 320 °C under pressure of 2 MPa. The liquefied products were analyzed with gas chromatograph (GC-7900) equipped with a SE-30 capillary column and a flame ionization detector. The temperatures of injector, column and detector were 280, 200 and 250 °C, respectively. Finally, the liquid products were analyzed through external standard method.

The conversion of aniline can be calculated by the following formula.

$$X_{\text{AN}} = \frac{n(\text{AN}_{\text{consume}})}{n(\text{AN}_{\text{consume}}) + n(\text{AN}_{\text{residue}})} \times 100\% \quad (1)$$

where $n_{\text{AN}_{\text{consume}}}$ and $n_{\text{AN}_{\text{residue}}}$ is the consumption and the remaining of the aniline, X_{AN} represents the conversion of aniline. The literature have reported that when LHSV was lower than 2 h^{-1} , a small amount of by-products such as *tmethylpyridine*, *p-toluidine* appeared [20]. Under laboratory reaction conditions (320 K, 2 MPa, LHSV at 2 h^{-1}), the selectivity was measured at 100% due to the very low content of by-products through the gas chromatography analysis.

2.3 Catalyst characterization

2.3.1 N_2 adsorption–desorption isotherm

The specific surface area, pore structure, and pore size of the sample were determined using the JW-ZQ 200 adsorption instrument (Beijing JWGB Sci & Tech Co., Ltd.). The specific surface area is calculated by the BET method, the adsorption–desorption isotherm is obtained by the volume method, and the pore size distribution is obtained

Table 1 Standard free energy of formation and standard enthalpy of formation

Substance	$\Delta_f G^0(\text{g})(\text{KJ/mol})$	$\Delta_f H^0(\text{g})(\text{KJ/mol})$	$S^0(\text{g})(\text{J/mol K})$
Aniline	129.7	82.6	
Diphenylamine	101.0	130.6	
Phenyl			40.6
Amino			18.0
Ammonia	- 16.4	- 45.9	

by density functional theory. High-purity nitrogen is the adsorbate and the operating temperature is $-196\text{ }^\circ\text{C}$.

2.3.2 X-ray diffraction

The structure of the phase is determined by X-ray diffraction (XRD). The light source is Cu $K\alpha$ rays, of which Cu target, $K\alpha$ is the ray source, the wavelength is 0.154 nm, the acceleration voltage is 40 kV, the tube current is 100 mA, the scan rate is 0.02°/s, and the scan range: $2\theta = 5^\circ\text{--}80^\circ$.

2.3.3 Py-IR

The acid properties and amount of Bronsted acid (BAS) and Lewis acid (LAS) were analyzed using Fourier transform infrared spectroscopy (Py-IR) with pyridine as the probe molecule. The instrument was Nicolet IS-10 which was equipped with a situ reaction cell. The infrared spectrum information of the samples was recorded at 200 °C and 450 °C to characterize the properties of total acid sites and strong acid sites. Their difference represents the weak acid sites. The quantity of Lewis acidic site and Bronsted acidic site was based on Lambert–Beer law: $A = \epsilon \cdot C \cdot d$ where ϵ is extinction coefficient, A is the corresponding absorbance, C is the concentration of the sample, and d represents the sample thickness. For pyridine, $\epsilon_{\text{Bronsted}}(1541\text{ cm}^{-1}) = 1.02\text{ cm}/\mu\text{mol}$ and $\epsilon_{\text{Lewis}}(1443\text{--}1453\text{ cm}^{-1}) = 0.89\text{ cm}/\mu\text{mol}$ have been employed to deduce the amount of Brønsted and Lewis acid sites, respectively.

3 Results and discussion

3.1 Thermodynamic analysis

In this paper, the thermodynamic analysis of the condensation reaction of aniline [21] was carried out. The reaction formula is shown in Scheme 1. The standard free energy of formation and the standard enthalpy of formation under the standard conditions of aniline, ammonia and diphenylamine can be found in the chemical manual [22]. The enthalpy

Table 2 Benson method to calculate the heat capacity of a substance

Substance	$C_p/\text{J}(\text{mol K})^{-1}$			
	400 K	600 K	800 K	1000 K
Aniline	143.00	192.80	225.10	230.90
Ammonia	13.06	21.35	28.30	32.98
Phenyl	21.81	26.45	27.33	27.46
Amino	38.70	45.30	51.10	56.20
Diphenylamine	56.68	74.25	82.96	87.90

Table 3 The relationship between material heat capacity and temperature

Substance	$C_p = A + BT^2 + CT^3 + DT^4$			
	A	B	C	D
Aniline	69.41	7.47×10^{-4}	-8.07×10^{-7}	2.21×10^{-10}
Diphenylamine	22.74	4.10×10^{-4}	-5.95×10^{-7}	2.50×10^{-10}
Ammonia	29.74	9.04×10^{-5}	-1.01×10^{-7}	3.67×10^{-11}

Table 4 Enthalpy change and Gibbs free energy change and equilibrium constant of reaction at different temperatures

	Temperature				
	280	300	320	340	360
$\Delta_r H(\text{g})$	- 77.85	- 80.82	- 83.94	- 87.21	- 90.63
$\ln K_{i,T}$	78.25	69.62	62.53	56.71	51.96
$\Delta_r G_{i,T}(\text{g})$	- 182.17	- 173.67	- 166.37	- 160.32	- 155.54

value is estimated based on the Joback group contribution method [23]. The results are listed in Table 1.

The heat capacity of diphenylamine is estimated based on the Benson group contribution method [24]. The results are shown in Table 2. According to the heat capacity of diphenylamine at different temperatures (400 K, 600 K, 800 K, 1000 K), the relationship between the heat capacity and temperature can be obtained, and the results are listed in Table 3. The change in heat capacity of other substances aniline and ammonia with temperature can be found in the literature [22].

According to the thermodynamic data of each substance involved in the reaction, the equilibrium constant and Gibbs free energy of each reaction are calculated using (2–4), the enthalpy change and Gibbs free energy change and equilibrium of the aniline condensation reaction at a specific temperature constant values are listed in Table 4.

$$K_{i,298} = e^{-\Delta_r G_{i,298}(\text{g})/RT} \quad (2)$$

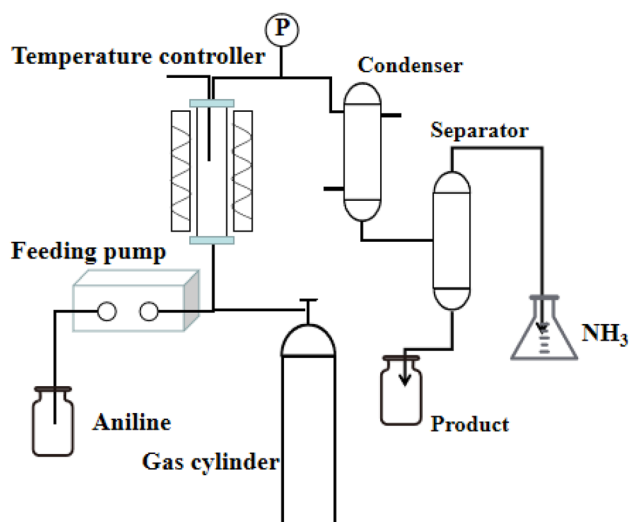


Fig. 1 Schematic view fixed-bed tubular reactor for the liquid phase conversion of aniline to diphenylamine

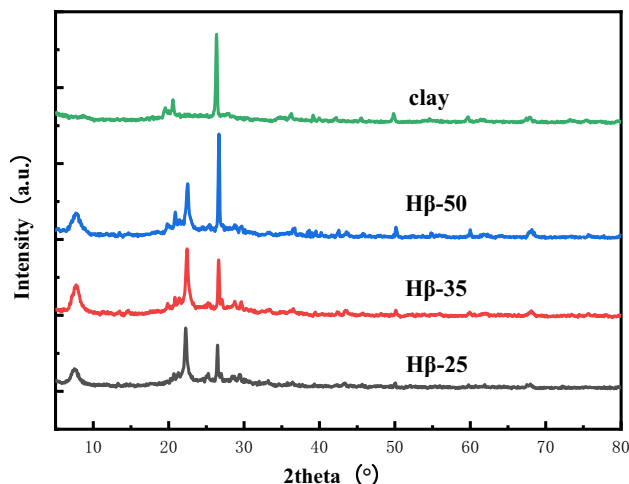


Fig. 2 XRD patterns of the Hβ-25, Hβ-35, Hβ-50, clay catalysts

$$\ln K_{i,T} = \ln K_{i,298} - \frac{\Delta rH_{i,T(g)}}{RT} \Big|_{298}^T \quad (3)$$

$$\Delta rG_{i,T(g)} = -RT \ln K_{i,T} \quad (4)$$

It can be seen from Table 4 that the condensation of aniline with diphenylamine is an exothermic reaction, indicating that high temperature operation is unfavorable for the reaction. The Gibbs free energy of the reaction at all temperatures is less than 0, which shows that the reaction is thermodynamically very favorable reaction.

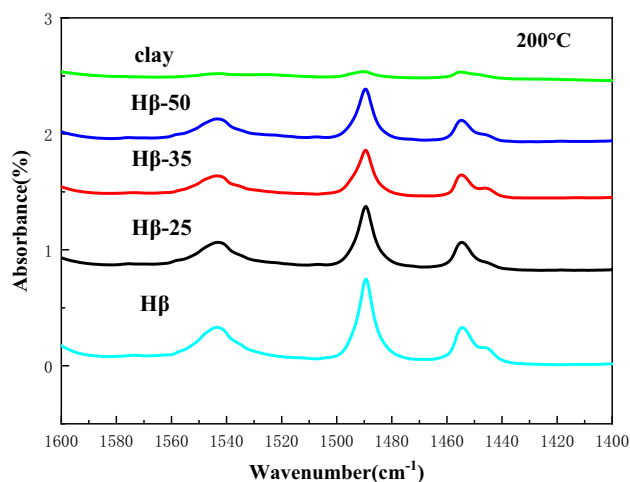


Fig. 3 All acid sites of the Hβ-25, Hβ-35, Hβ-50, clay catalysts

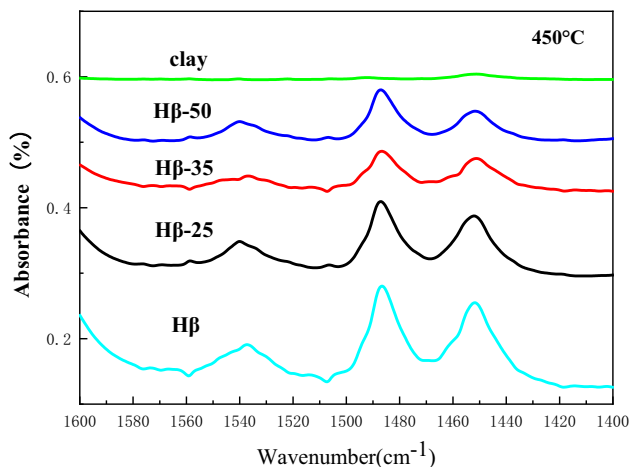


Fig. 4 Strong acid sites of the Hβ-25, Hβ-35, Hβ-50, clay catalysts

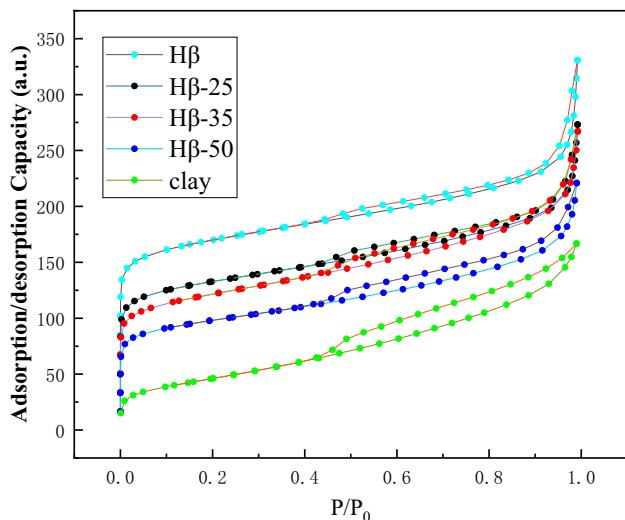
3.2 Catalyst characterization

3.2.1 Structural properties

The XRD patterns of the Hβ zeolite with different clay loadings (Hβ, Hβ-25, Hβ-35, Hβ-50, clay) were shown in Fig. 2. It can be observed that all the samples exhibit the same diffraction peaks in the scopes of $2\theta = 7^\circ - 9^\circ$ and $21^\circ - 22.5^\circ$, matching well with the standard phase of β zeolite. The peak around $2\theta = 26^\circ$ is geared to the clay. With the amount of clay loading is increasing, the intensity of peaks corresponding to clay adds up, relatively. Simultaneously, the intensity of peaks corresponding to β zeolite decreased. This is due to a progressively lower fraction of zeolite and progressively increasing fraction of clay in the measured samples.

Table 5 Acid sites distribution in catalysts monitored by Py-IR

Sample	LAS ($\mu\text{mol/g}$)			BAS ($\mu\text{mol/g}$)		
	Weak	Strong	Total	Weak	Strong	Total
H β	56	54	110	275	37	312
H β -25	35	40	75	131	28	159
H β -35	43	21	64	106	14	120
H β -50	35	15	50	96	12	108
Clay	17	5	22	38	0	39

**Fig. 5** Isotherms adsorption–desorption of H β -25, H β -35, H β -50, clay catalysts

3.2.2 Chemical analysis

The Py-IR spectra of H β zeolite with different clay (H β , H β -25, H β -35, H β -50, clay) loadings were shown in Figs. 3 and 4. The peaks ascribed to LAS and BAS are observed at 1450 cm^{-1} and 1540 cm^{-1} respectively. The pyridine adsorbed at $200\text{ }^{\circ}\text{C}$ can be taken as a quantitative measure of total acid sites presenting in the samples while the desorption at $450\text{ }^{\circ}\text{C}$ measures strong acid sites quantitatively. And their difference was the weak acids.

The condensation of aniline to diphenylamine is a typical acid-catalyzed reaction. For this reason, the amount of acid was a vital parameter in the activity of the catalyst. As

exhibited in Table 1, H β zeolite displayed the largest amount of acid in Lewis acid as well as Bronsted acid sites while clay was the smallest. Additionally, there was a gradual decrement in acid sites due to the loading of clay. Therefore, it can be concluded that the loading of clay will result in the reduction of acid sites. According to the results collected in Table 5, whether in Lewis or Bronsted acid sites, the weak, strong and total acid sites decreased continuously as the amount of clay increased. Compared to the strong acid sites, the weak acid sites accounted for the main part either in Lewis or Bronsted acid sites, particularly in clay.

3.2.3 Textural properties

The structural properties of H β zeolite with different clay (H β , H β -25, H β -35, H β -50, clay) loadings were listed in Fig. 5 and Table 6. Mesopore volume was the difference between V_{total} and V_{micro} . The materials, according to the IUPAC classification, exhibit combined type I and IV isotherms. All samples displayed a high N_2 uptake at low (P/P_0) due to micropore filling. The isotherm of the parent material was close to a type I isotherm typical of a microporous solid, with a rather horizontal hysteresis loop, indicating a low volume of mesopores with a broad pore size distribution. H β zeolite with 50% clay and pristine clay exhibited a more pronounced type IV isotherm contribution, which is a characteristic of mesoporous materials. As the amount of clay loading on the H β increased, the micropore surface area of the H β decreased evidently. In contrast, there was a significant increment in the ratio of meso surface area and micropore surface. Larger surface area and pore size are beneficial to increase the mass transfer rate of the reaction and reduce the formation of carbon deposits. As what could

Table 6 Physical properties of H β -25, H β -35, H β -50, clay catalysts

Catalyst	S_{BET} (m^2/g)	S_{micro} (m^2/g)	S_{meso} (m^2/g)	$S_{\text{meso}}/S_{\text{micro}}$	V_{total} (cm^3/g)	V_{micro} (cm^3/g)	V_{meso} (cm^3/g)	PD (nm)
H β	556	400	155	0.39	0.49	0.20	0.29	3.50
H β -25	422	272	150	0.55	0.40	0.14	0.26	3.81
H β -35	398	225	173	0.77	0.39	0.11	0.28	3.92
H β -50	309	166	142	0.85	0.34	0.09	0.25	4.39
Clay	167	0	167	–	0.26	0.00	0.26	6.16

be seen in Table 6, the total and micro specific surface area of H β zeolite was 556 m²/g and 400 m²/g respectively. The value of clay was 167 m²/g and 0. The total and micro surface area of the synthetic composite decreased gradually as the loading of clay increased while the ratio of micro surface area to meso surface area increased. We can suppose that the loading of clay influenced the distribution of micropores and mesopores. Correspondingly, the total and micro volume decreased with the increase loading of clay. Moreover, the composite enhanced porous structure with an average pore diameter as compared to 6.16 nm and 3.50 nm for bentonite and β zeolite.

3.3 Catalytic performance

3.3.1 Laboratory experiment

A comparative catalytic study on different amount of clay was conducted at 320 °C under 2 MPa with LHSV of 2 h⁻¹. Catalytic performance of β zeolite with different clay loading

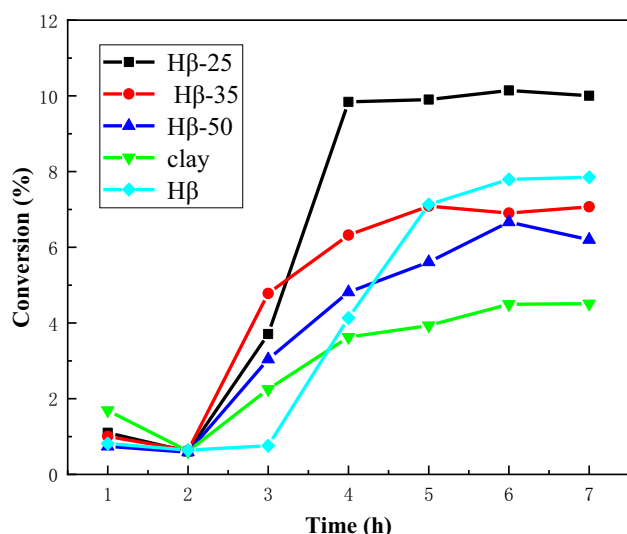
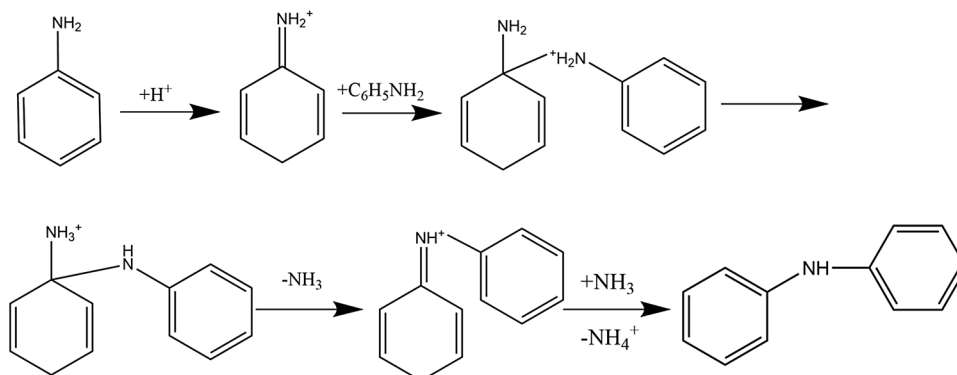


Fig. 6 Catalytic performance of β zeolite with different clay loading

was shown in Fig. 6. The selectivity of product was 100% as mentioned above. As appeared in the plotted curves, the conversion of aniline catalyzed by raw H β zeolite remained low in the first 2 h, increased rapidly from the 3rd to the 5th h and reaching about 8% in the last 2 h. The clay had the same tendency as a catalyst, and finally reached a conversion rate of about 4%. Whether in amount of acid sites or surface area, H β zeolite was higher than that of clay, which gave rise to the better catalytic performance of H β zeolite. The conversion of aniline that adopted the composite as a catalyst was increasing continuously during the first 4 h on stream and stabilized after that gradually. As the reaction progressed continuously, the high temperature would lead the catalyst to deactivate carbon deposits. Or the reactant product blocked the pipeline, which is not conducive to the reaction.

As the amount of clay increased to 25%, the conversion has increased dramatically. The H β zeolite loaded with 25% clay exhibited the highest conversion which achieved 10%. The further increase in the loading of clay was of a negative impact and resulted in the reduction of the conversion of aniline. This was determined by the physical properties such as the specific surface and pore size of various catalysts and the chemical properties such as the acid strength and acid amount of the active center. The amount of acid sites and surface area decreased to a certain extent, indicating that the catalytic performance was related to them. In addition, the kinetic diameter of aniline and diphenylamine are close to the pore size of the zeolite. The pore size of the zeolite has a significant effect on the selectivity of diphenylamine. Smaller pore size is not conducive to the formation and diffusion of diphenylamine. And also, through the exploration of the reaction mechanism and quantum chemistry calculations, Bochkarev et al. [5] found that the synthesis of intermediate products is the control step of the reaction rate. The mechanism was shown in Fig. 7. Accordingly, clay plays a crucial role in the catalytic reaction. It introduces mesopores, changes the pore structure of the catalyst, and increases the meso specific surface area. Added mesopores make the diffusion of intermediate products easier, and thereby promote the reaction. To summarize, the H β zeolite

Fig. 7 Catalytic reaction mechanism of condensation of aniline to diphenylamine [5]



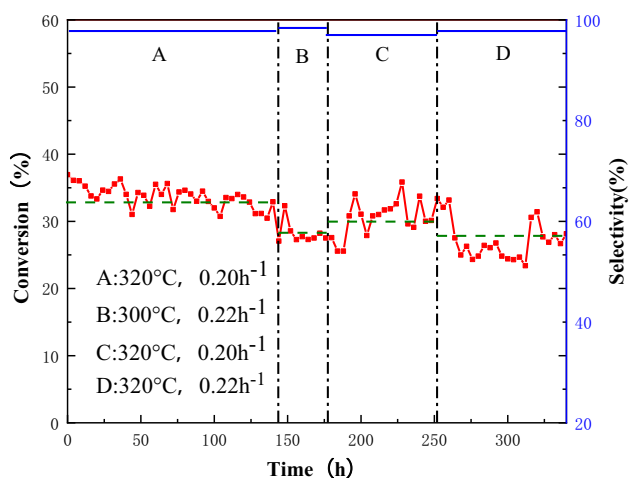


Fig. 8 Stability test of catalysts for aniline condensation

loaded with 25% clay have succeeded in our main goal to enhance the conversion of the reaction.

3.3.2 Pilot test

In order to evaluate the lifetime of the catalyst, we simulated the industrial process to test the stability of the catalyst loaded with 25% clay for up to 340 h. The reaction was conducted at 315–320 °C with a liquid hourly space velocity (LHSV) of 0.20–0.22 h⁻¹. And the experiment at the pilot scale was carried out in a 180 ml device. The stability test results were shown in Fig. 8. During the reaction process, we changed the operating conditions to investigate the effect of temperature and space velocity on the activity. The test was divided into four parts according to the reaction time, namely zone A (0–140 h, 320 °C, 0.20 h⁻¹), B (140–176 h, 315 °C, 0.22 h⁻¹), C (176–252 h, 320 °C, 0.20 h⁻¹), D (252–340 h, 320 °C, 0.22 h⁻¹). As shown in Fig. 8, the order of average conversion of aniline from high to low is: A (33.75%) > C (31.35%) > B (27.64%) > D (26.35%). At the beginning of the reaction (zone A), the average conversion was 33.75% while the selectivity reached 97.06%. It could be seen that a small amount of by-product will be produced at low LHSV. In zone B, we investigated the effects of temperature and space velocity on conversion and selectivity. The average conversion dropped slightly and the selectivity was 97.64%. After restoring the initial process conditions (zone C), catalytic activity has rebounded. The conversion has risen back to 31.65% and the selectivity was 96.58%. As LHSV increased, the conversion rate decreased again. It is well known that the catalyst at higher temperature and lower LHSV displayed higher catalytic activity. With the progress of the reaction, the conversion rate and selectivity fluctuated in a small range, showing good catalyst stability.

4 Conclusions

β zeolite/bentonite was synthesized and applied effectively in the condensation of aniline to diphenylamine. The XRD, N₂ adsorption–desorption and acidity analysis results confirmed that surface area and the acidity distribution are both related to the conversion of aniline. The N₂ adsorption/desorption experiment showed that the loading of clay increased the mesoporous area. And it had been found that with an increasing amount of clay loading, the intensity of peaks corresponding to β zeolite decreased from the XRD pattern. In addition, it was revealed by Py-IR that the catalyst which was loaded with 25% clay shows higher acidity than others. The mesopores that clay brought in accelerated the diffusion of the intermediate and promoted the condensation. Moreover, the amount of acid decreased with the increasing loading of clay. The results also showed that when 25% clay is loaded with zeolite, the catalyst displayed high performance (the conversion of 9.90%) compared with that of H β zeolite (the conversion of 7.85%) and clay (the conversion of 4.49%). At last, the catalyst at the pilot scale displayed good stability as well.

References

1. M. Hronec, Z. Cvenrošová, J. Čejka, Synthesis of diphenylamine catalyzed by zeolites. *Appl. Catal. A* **255**, 197–202 (2003)
2. O. Immel, H. Waldmann, R. Langer, G. Darsow, H.-J. Buysch, Process for the preparation of diphenylamines. EP Patent 0526793 (1993)
3. T. Nagata, C. Kusuda, M. Wada, Process for the preparation of diphenylamine or nucleus-substituted derivative thereof. US Patent 5545752 (1996)
4. V.D. Stytsenko, T.D. Hyu, V.A. Vinokurov, Kinetics and mechanism of diphenylamine synthesis by the condensation of aniline with oxygen-containing compounds. *Kinet. Catal.* **48**, 292–297 (2007)
5. V.V. Bochkarev, L.S. Soroka, T.A. Klimova, L.E. Velikorechina, Modeling of condensation reaction of aniline to diphenylamine by PM7 method. *Procedia Chem.* **15**, 320–325 (2015)
6. A. Salem, R. Akbari Sene, Removal of lead from solution by combination of natural zeolite–kaolin–bentonite as a new low-cost adsorbent. *Chem. Eng. J.* **174**, 619–628 (2011)
7. K. Tarach, K. Góra-Marek, J. Tekla, K. Brylowska, J. Datka, K. Mlekodaj, W. Makowski, M.C. Igualada López, J. Martínez Triguero, F. Rey, Catalytic cracking performance of alkaline-treated zeolite beta in the terms of acid sites properties and their accessibility. *J. Catal.* **312**, 46–57 (2014)
8. B.O. Dalla Costa, M.A. Peralta, C.A. Querini, Gas phase dehydration of glycerol over, lanthanum-modified beta-zeolite. *Appl. Catal. A* **472**, 53–63 (2014)
9. N. Blanch-Raga, A. Palomares, J. Martínez-Triguero, S. Valencia, Cu and Co modified beta zeolite catalysts for the trichloroethylene oxidation. *Appl. Catal. B* **187**, 90–97 (2016)
10. M.A. Cambor, A. Corma, S. Valencia, Spontaneous nucleation and growth of pure silica zeolite- β free of connectivity defects. *Chem. Commun.* (1996). <https://doi.org/10.1039/CC9960002365>

11. A. Corma, L.T. Nemeth, M. Renz, S. Valencia, Sn-zeolite beta as a heterogeneous chemoselective catalyst for Baeyer-Villiger oxidations. *Nature* **412**, 423–425 (2001)
12. V.V. Bochkarev, L.s. Soroka, Investigation of the role catalysts in the condensation of aniline to diphenylamine. *Bull. Tomsk Polytech. Univ.-Geo Assets Eng.* **314**, 93–97 (2009)
13. S.A. Ali, F.M. Almulla, B.R. Jermy, A.M. Aitani, R.H. Abudawoud, M. AlAmer, Z.S. Qureshi, T. Mohammad, H.S. Alasiri, Hierarchical composite catalysts of MCM-41 on zeolite beta for conversion of heavy reformat to xylenes. *J. Ind. Eng. Chem.* **98**, 189–199 (2021)
14. A. Tishin, U. Krut, O. Tishina, E. Beskhmel'nitsyna, V. Yakushev, Physico-chemical properties of montmorillonite clays and their application in clinical practice (review). *Res. Results Pharmacol.* (2017). <https://doi.org/10.18413/2313-8971-2017-3-3-37-54>
15. S. Ghonem, M. Abukhadra, Synthesis of Na + trapped bentonite/zeolite-P composite as a novel catalyst for effective production of biodiesel from palm oil; Effect of ultrasonic irradiation and mechanism. *Energy Convers. Manag.* **196**, 739–750 (2020)
16. S. Belkhiri, M. Guerza, S. Chouikh, Y. Boucheffa, Z. Mekhalif, J. Delhalle, C. Colella, Textural and structural effects of heat treatment and γ -irradiation on Cs-exchanged NaX zeolite, bentonite and their mixtures. *Microporous Mesoporous Mater.* **161**, 115–122 (2012)
17. M. Budihardjo, F. Muhammad, A. Rizaldianto, E. Sutrisno, I. Wardhana, in *Stability performance of the mixture of bentonite and zeolite as landfill liner*, E3S Web of Conferences, vol. 125, (2019), p. 07012
18. M. Shaban, M.R. Abukhadra, M.G. Shahien, S.S. Ibrahim, Novel bentonite/zeolite-NaP composite efficiently removes methylene blue and Congo red dyes. *Environ. Chem. Lett.* **16**, 275–280 (2018)
19. M.R. Abukhadra, S.M. Ali, A.M. El-Sherbeeney, A. Soliman, A. Elgawad, Effective and environmental retention of some radioactive elements (U(VI), Sr(II), and Ba(II)) within bentonite/zeolite hybrid structure; equilibrium and realistic study. *Inorg. Chem. Commun.* **119**, 108053 (2020)
20. M. Radhakrishnan, B. Das, D. Nandi, ChemInform Abstract: high pressure synthesis of diphenylamine from aniline and phenol. *Chem. Inform.* (1983). <https://doi.org/10.1002/chin.198333165>
21. V.V. Bochkarev, N.P. Romanenko, L.s. Soroka, Thermodynamic analysis of the process condensation of aniline to diphenylamine. *Russ. Chem. Ind.* **11**, 12–15 (2002)
22. W. Haynes, *CRC Handbook of Chemistry and Physics* (CRC Press, Boca Raton, 2012)
23. L. Yinghua, M. Peisheng, L. Ping, Estimation of liquid viscosity of pure compounds at different temperatures by a corresponding-states group-contribution method. *Fluid Phase Equilib.* **198**, 123–130 (2002)
24. N. Thangarajoo, S.A.A. Taqvi, P. Matheswaran, K. Johari, M.H. Noh, Prediction of infinite dilution activity coefficient of alcohol in ionic liquids using group contribution method. *J. Mol. Liq.* **324**, 114723 (2021)

Publisher's Note Springer Nature remains neutral with regard to jurisdictional claims in published maps and institutional affiliations.